JACS
JOURNAL OF THE AMERICAN CHEMICAL SOCIETY

ARTICLE

pubs.acs.org/JACS

Controlling Chain Conformation in Conjugated Polymers Using Defect Inclusion Strategies

Giannis Bounos,[†] Subhadip Ghosh,[†] Albert K. Lee,[†] Kyle N. Plunkett,[‡] Kateri H. DuBay,[‡] Joshua C. Bolinger,[*,†] Rui Zhang,[†] Richard A. Friesner,[‡] Colin Nuckolls,[‡] David R. Reichman,[‡] and Paul F. Barbara[†]

[†]Department of Chemistry and Biochemistry and the Center for Nano and Molecular Science and Technology, University of Texas, Austin, Texas 78712, United States

[‡]Department of Chemistry, Columbia University, 3000 Broadway, New York, New York 10027, United States

Supporting Information

ABSTRACT: The Horner method was used to synthesize random copolymers of poly(2-methoxy-5-(2′-ethylhexyloxy)-*p*-phenylene vinylene) (MEH-PPV) that incorporated different backbone-directing monomers. Single-molecule polarization absorption studies of these new polymers demonstrate that defects that preserve the linear backbone of PPV-type polymers assume the highly anisotropic configurations found in defect-free MEH-PPV. Rigid defects that are bent lower the anisotropy of the single chain, and saturated defects that provide rotational freedom for the chain backbone allow for a wide variety of possible configurations. Molecular dynamics simulations of model defect PPV oligomers in solution demonstrate that defect-free and linearly defected oligomers remain extended while the bent and saturated defects tend toward more folded, compact structures.

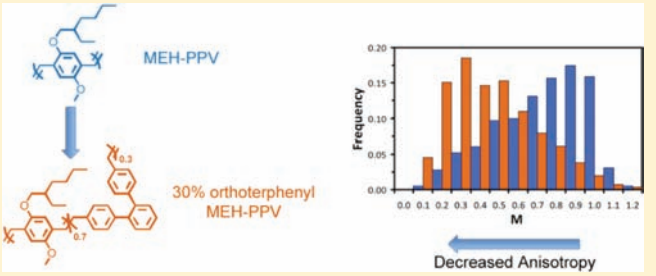

INTRODUCTION

With the increasing interest in conjugated polymers and their use in low-cost, easily processed devices such as organic light-emitting diodes (OLEDs), photovoltaics, and field effect transistors, understanding the role that morphology plays in the electronic properties and long-term stability of these devices is critical to creating better materials.[1−4] Discerning how the structure of a single chain evolves from a single molecule to a thin film, a bulk heterojunction or even a higher-order structure will lead to key insights for molecular design strategies. The single chain structure has long been a topic of interest.[5−10] Over the course of the past decade, numerous studies have provided evidence that the prototypical conjugated polymer poly(2-methoxy-5-(2′-ethylhexyloxy)-*p*-phenylene vinylene) (MEH-PPV), when isolated in a matrix of PMMA, can assume a myriad of configurations ranging from highly amorphous structures such as the "molten globule" and "defect cylinder" to highly ordered ones such as the "toroid" and "rod".[11] Recent improvements in synthetic methods, polymer purification techniques, and optical characterization have shown that MEH-PPV chains uniformly fold into highly anisotropic rod-like structures, as proposed previously.[5]

Recent work has demonstrated that synthetic strategies to incorporate saturated backbone defects can disrupt the nature of polymer backbone folding by acting as kinks in the rigid PPV chain. Polarization anisotropy measurements and simulations show that higher defect inclusion rates lower the anisotropy values measured for these conjugated systems.[11] In these previous studies, the vinyl linkages in the PPV backbone were randomly saturated resulting in a truncation of the chromophores in the chain. This leads to a blue shift of the solution absorption spectra by an amount dictated by the degree of backbone saturation and concomitantly limits the range of energy funneling that occurs in typical conjugated polymer molecules.[12] In comparison to recent results,[5] the discrepancies between older synthetic efforts and today's commercially available materials deserves attention as well as more refined techniques aimed at polymer conformational control. It is natural to ask if, with proper synthetic techniques, one can controllably alter the conformation of a single polymer chain in a controlled and systematic manner characterizable by single molecule and theoretical methods. In this study, we measure the polarization anisotropy of single polymer chains with a variety of "morphology directing" inclusions of different concentrations. These "defects" include groups that preserve the high anisotropy originally observed in MEH-PPV, rigid groups that result in very low anisotropy conformations, and a flexible group that allows for a broad distribution of observable anisotropies. Molecular dynamics simulations have been performed on oligomers of "defected" MEH-PPV to provide insight into the role that defects play on the local folding of the polymer chain in solution. This collaborative effort thus demonstrates a powerful synthetic approach for polymer morphology control.

Received: February 10, 2011
Published: May 25, 2011

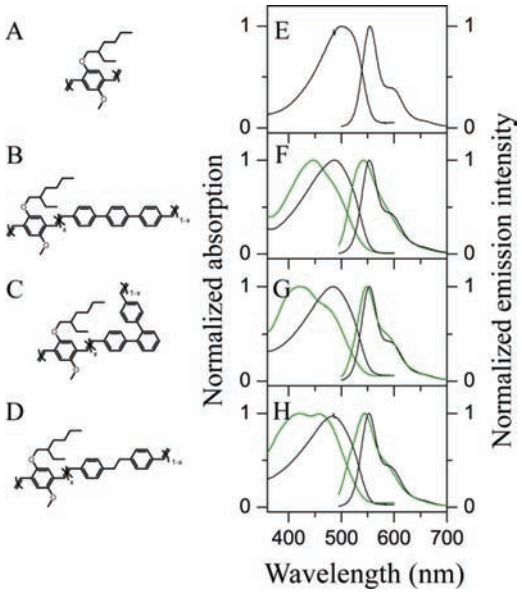

Figure 1. (A−D) Chemical structures of the conjugated polymers: MEH-PPV, para-terphenyl MEH-PPV, ortho-terphenyl MEH-PPV, and saturated MEH-PPV, respectively. (E−H) Absorption and emission spectra of the corresponding polymers are shown to the left. In (F−H), 10% defect inclusion is represented in black lines, and 30% defect inclusion is represented in green lines.

RESULTS AND DISCUSSION

Solution Absorption and Emission Spectra. The chemical structures of MEH-PPV and the defect copolymers are shown in the left side of Figure 1A−D and each compound's corresponding solution phase absorption and emission spectra on the right side (Figure 1E−H), with (A) MEH-PPV, (B) para-terphenyl defected MEH-PPV (para-terphenyl MEH-PPV), (C) ortho-terphenyl defected MEH-PPV (ortho-terphenyl MEH-PPV), and (D) 1,2-diphenylethane defected MEH-PPV (saturated MEH-PPV). The para-terphenyl defect is a stiff linear molecule that is expected to maintain the linearity of the PPV backbone; the ortho-terphenyl defect is a highly kinked species that should disturb the ordering of the pristine polymer, and the saturated defect lends rotational flexibility to the polymer backbone. The absorption maximum of defect-free MEH-PPV is 503 nm, in good agreement with previous work, while the 10% defected polymers each undergo substantial blue shifts (~20 nm), and the 30% defected polymers demonstrate shifts up to 80 nm dependent on defect type. Previous studies have shown that the absorption spectra of PPV type polymers are sensitive to the concentration of saturated defects along the polymer backbone with increased defects blue shifting the absorption to higher energies, consistent with our results.[12] Solution emission spectra for all defected species show only a modest change upon defect inclusion as shown in Figure 1. At 10% defect inclusion, emission spectra are almost identical to that of MEH-PPV, and even at 30% defect inclusion, the peak of emission is blue-shifted by <10 nm. Spectra at 30% are also broadened, masking the vibronic band shoulder. The fact that the emission spectra of the defected polymers are not blue-shifted suggests that even in the highly defected species there is still a subset of lower energy, longer chromophores present in each polymer chain, and energy transfer to these emitting sites remains efficient in solution.

NMR Analysis. MEH-PPV samples were prepared via the Horner condensation method (see Supporting Information), which has been shown to produce *trans* double bonds in preference to *cis* double bonds.[13] NMR characterization of the methylene resonances from the ethylhexyl group from 3.5 to 4.0 ppm provides a quantitative marker for determining the *cis*/*trans* ratio.[14,15] The methylene protons adjacent to *trans* double bonds arise at 3.9 ppm, while the methylene protons adjacent to a *cis* double bond appear at 3.5 ppm. Using these characterization strategies, MEH-PPVs prepared by the Horner method have consistently reported *cis* inclusion rates of 2−5%.[13−15] Our synthesized MEH-PPV, without the incorporation of defect sites, showed a similar *cis* double bond inclusion of 5.3%. However, we have found that including engineered defect sites in the polymer backbone can dramatically disturb the *cis*/*trans* ratio in MEH-PPV. For example, when preparing MEH-PPV with ortho-terphenyl defect groups at 10% or 30% defect loading, the *cis* double bond inclusion rate jumped to 18.7% and 13.1%, respectively. Similarly, when saturated defects were incorporated at 10% or 30% defect loading, the *cis* double bond inclusion rate was again high at 19.0% and 15.1%, respectively. The inclusion of para-terphenyl defects at 10% or 30% loading provided polymers with *cis* double bond inclusion rates of 5.8% and 7.6%, respectively, similar to that of the native MEH-PPV. We theorize that the incorporated defects template the polymerization and influence the chemical reaction pathway (i.e., formation of *cis* or *trans* double bonds). The para-terphenyl defect is a linear segment that does not undermine the linear *trans* double bonds of MEH-PPV, and therefore we see little change to the amount of *cis* inclusion. In contrast to the linear defect, the ortho-terphenyl defect installs a 60° kink in the polymer backbone. This structural modification disorients the polymer segments away from linearity and templates a more globular assembly. We suggest *cis* double bonds are incorporated at higher rates during polymerization to allow better intramolecular chain packing and reduce the overall energy. A similar result arises from incorporation of the conformationally flexible, saturated defect. During polymer growth the defects could provide a hinge-like segment that allows the polymer segments to bend onto itself, creating more *intra*-molecular associations. A globular structure can result that would warrant the inclusion of more *cis* defects. Finally, the *cis* double bond inclusion was slightly greater in MEH-PPVs with 10% defect inclusion than in 30% defect inclusion polymers.

Polarization Modulation Depth. The absorption polarization modulation was measured for ensembles of single polymer chains of MEH-PPV with the conformation directing groups discussed above as well as "pure" MEH-PPV for comparison. This method has been discussed in detail in previous studies.[5,11] In brief, using the microscope apparatus described in the supporting information, linearly polarized excitation is modulated such that the angle of polarization is rotated 180°. As the angle of the polarized light matches the orientation of a transition dipole in a fluorescent species, the increase in excitation rate becomes apparent from the increased fluorescence intensity. This interplay between fluorescence intensity and polarization angle, θ, is described by the following equation

$$I(\theta) \propto 1 + M\cos 2(\theta - \varphi)$$

where φ is the orientation when the emission intensity is maximized. M is the polarization modulation depth. For a single

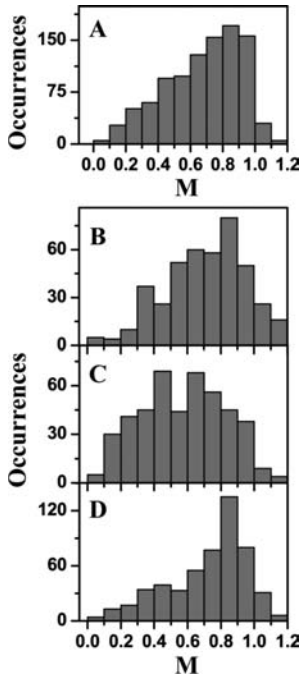

Figure 2. Experimental histograms of modulation depth, M, obtained with 488 nm excitation of (A) MEH-PPV (981 molecules), (B) 10% para-terphenyl MEH-PPV (424 molecules), (C) 10% ortho-terphenyl MEH-PPV (454 molecules), and (D) 10% saturated MEH-PPV (524 molecules).

dipole or a collection of dipoles with similar orientation, $M = 1$. For an isotropic distribution of dipoles where the spacing between dipoles is much smaller than the diffraction limit of light, $M = 0$; that is, no modulation should be observed.

In the case of a conjugated polymer such as MEH-PPV, a single chain consists of multiple chromophore segments, each composed of a set of sequential monomers, that are capable of absorbing light.[16] Recent polarization modulation measurements of defect-free MEH-PPV reveal a single distribution of modulation values centered at ~0.7, suggesting that each individual polymer is folding into a well-ordered structure in which the majority of the chromophore dipoles are aligned. The resulting distribution of observed modulation depth values is due to variation in single-chain folding from molecule to molecule and a lack of preferential orientation in the film where a molecule tilted out of the sample plane will have a smaller observed modulation depth than an identical molecule lying flat in the sample plane.[5] These results are qualitatively consistent with the picture that has emerged from coarse-grained Monte Carlo simulations of interacting beads on a chain.[5]

In this work, a 488 nm excitation was used to democratically interrogate the chromophores in the defect-free MEH-PPV as well as in the 10% defected MEH-PPV species, as this wavelength is near the peak of the solution absorption for these species (Figure 1). For the 30% defected MEH-PPV species, 488 nm excitation is on the red edge of the absorption spectrum and is therefore likely to excite only a lower-energy subset of chromophores, resulting in nondemocratic excitation of the polymer chain which artificially creates high anisotropy values (data shown in the Supporting Information, Figure S1). Therefore, 458 nm excitation was used to probe the 30% defected chains. Polarization modulation depth histograms for the defect-free MEH-PPV

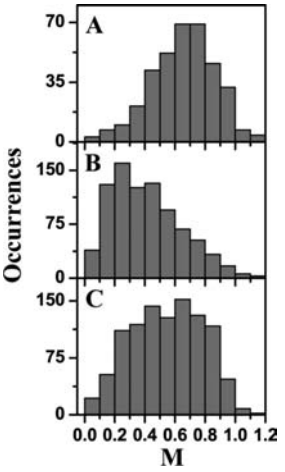

Figure 3. Experimental histograms of modulation depth, M, obtained with 457 nm excitation of (A) 30% para-terphenyl MEH-PPV (362 molecules), (B) 30% ortho-terphenyl MEH-PPV (862 molecules), and (C) 30% saturated MEH-PPV (1033 molecules).

and the 10% defected compounds in this study are presented in Figure 2, and the modulation depth histograms for the three 30% defected MEH-PPV compounds studied are presented in Figure 3. Although Figure 2 only presents results obtained with 488 nm excitation, excitation at 458 nm was also done, resulting in the same general trends for the modulation depth distributions with an ensemble average modulation depth slightly lower than that obtained at 488 nm (data shown in the Supporting Information, Figure S2).

Molecular Dynamics. Replica exchange molecular dynamics (REMD)[17] was used to probe the canonical ensemble of structures at 300 K for a set of 10 oligomer variants for each type of defect (30% defected) as well as five oligomer variants for the defect-free MEH-PPV (see Supporting Information for details), all starting from extended configurations. Representative structures for the various chains, chosen to display a range of anisotropies, are shown in Figure 4, as are the average radii of gyration, anisotropy order parameters, and modulation depths. Two particularly noteworthy structures are also shown in Figure 5.

Radii of gyration are calculated from the coordinates of just the initial carbon atom from each monomer, as are the vectors representing the orientation of the chain between each monomer. A set of 15 atom coordinates is therefore used to calculate the center of mass and then the distances contributing to the radius of gyration for each structure, and a corresponding set of 14 vectors is used to determine the anisotropy for each structure. Statistics are calculated on 400 structures from each REMD run, from structures obtained at regular intervals for the last 4 ns of each 5 ns run. The anisotropy order parameter, A, is determined from $A = (3S_c)/(2 + S_c)$, and S_c, the order parameter of the polymer chain, is calculated as $S_c = 0.5\langle 3(\cos^2 \beta) - 1\rangle$, where the angled brackets indicate an average over the full set of chain vectors for each structure and β is the angle between each chain vector and the principal internal axis of those vectors.[5] A value of $A = 1.0$ indicates complete alignment of the chain vectors while a value of $A = 0.0$ indicates no alignment. The distribution of anisotropies was then converted to a distribution of modulation depths to better compare to the experimentally measured values, as described in ref 5. Average values of the radius of gyration, the

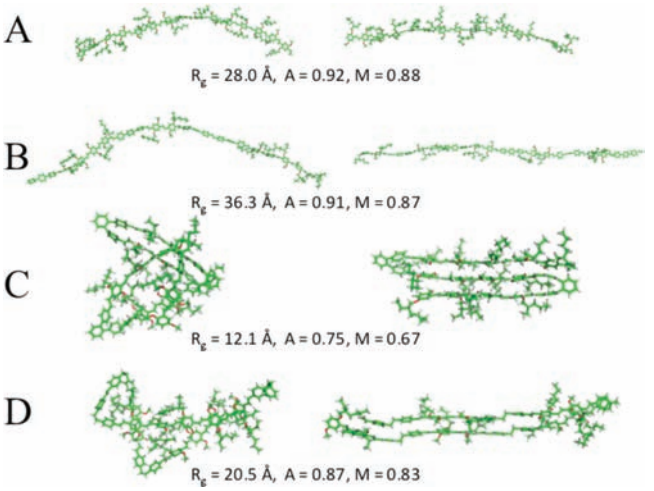

Figure 4. Representative molecular structures from REMD simulations of short 15 unit oligomers of (A) MEH-PPV, (B) ~33% para-terphenyl MEH-PPV, (C) ~33% ortho-terphenyl MEH-PPV, and (D) ~33% saturated MEH-PPV. The corresponding radius of gyration, anisotropy order parameter, and modulation depths are also shown. See the Molecular Dynamics section for details.

anisotropy order parameter, and the corresponding modulation depths were then calculated.

The simulations were done both in implicit toluene and in the gas phase (data not shown), and the resulting structures were quite similar. This suggests that mean field solvation effects do not greatly influence the stability and internal alignment of these collapsed oligomers at 300 K. However, it is important to note that both toluene and gas-phase simulations neglect the effect of PMMA, the carrier polymer, as well as the entire spin-casting process, on the final morphology of the spin-cast conjugated polymers. Such effects are not negligible, especially in light of recent work demonstrating significant changes in polymer morphology when toluene solvent vapor annealing is performed on single molecule MEH-PPV/PMMA systems.[10] Results shown are from all-*trans* oligomers in implicit toluene, and their statistics are calculated over the set of five unique polymer sequences where defects were placed probabilistically (see Supporting Information) for both the nondefected MEH-PPV and the defected MEH-PPV chains.

Defect-Free MEH-PPV. Figure 2A presents modulation depth data for 16 kDa (~60 monomer length chain) MEH-PPV without defects present. Consistent with previous results from studies done on MEH-PPV with a higher molecular weight, modulation depths for these shorter, defect-free, MEH-PPV chains are distributed around a single value with an average modulation depth of 0.67. One important difference to note in this work as compared to the previous studies on longer MEH-PPV chains is the increased signal-to-noise ratio for these very low molecular weight chains. As more error is introduced into the measurement, the modulation depth histograms become broader, as can be seen in the increased number of molecules with modulation depths above the physically realistic value of one as compared to previous studies.[5,10−12] As can be seen in Figure 4A, the defect-free MEH-PPV oligomer demonstrated no propensity to fold during the course of the REMD simulations, adopting instead an elongated conformation with only slight fluctuations away from linear configuration. The resulting radius of gyration is rather large, at 28.0 Å, and the anisotropy order parameter is also quite high, with a value of 0.92 and a corresponding average modulation depth of 0.88. Such stiff chains will nonetheless fold at longer chain-lengths,[11] but the stiffness demonstrated in these oligomers suggest that it will be favorable for these molecules, even once folded, to adopt a set of stiff, highly ordered, and anisotropic configurations qualitatively consistent with the single molecule data shown above.

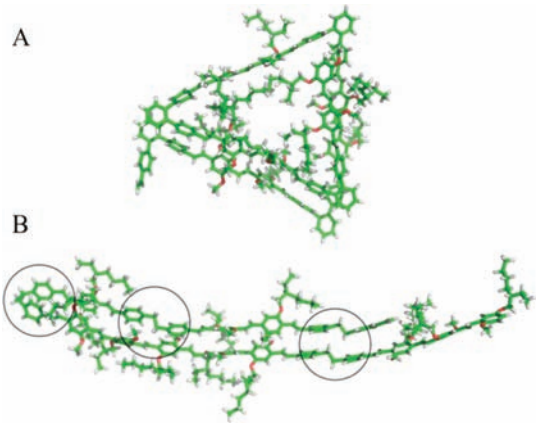

Figure 5. Additional structures of (A) ~33% ortho-terphenyl MEH-PPV and (B) ~33% saturated MEH-PPV. Saturated defects discussed in the text are circled in B.

Para-Terphenyl MEH-PPV. This linear defect preserves the extended, stiff backbone configuration common to PPV polymers and is not expected to introduce dramatic changes in the polymer's overall morphology. Indeed, the modulation depth histograms of both 10% and 30% para-terphenyl MEH-PPV (Figures 2B and 3A) present nearly identical distributions in both their shape and average modulation depth (0.67 and 0.64, respectively) to that of the defect-free MEH-PPV. Likewise, the structures that are observed during our simulations of 33% para-terphenyl MEH-PPV (Figure 4B) are also quite similar to those for the defect-free MEH-PPV, although elongated since a single para-terphenyl group is longer than the corresponding MEH-PPV monomer. The radius of gyration (36.3 Å) is therefore greater, but the anisotropy order parameter (0.91) and the modulation depth (0.87) are nearly the same. These results together confirm our hypothesis that a stiff, linear defect would preserve the highly anisotropic nature of the single-molecule MEH-PPV morphology. The only observed effect of the para-terphenyl defect inclusion in our study, namely, the shift in peak absorption, can be attributed to the corresponding disruption to the average conjugation length, since the π conjugation is reduced by the nonplanar geometry of the phenyl rings in the terphenyl group.[18]

Ortho-terphenyl MEH-PPV. Ortho-terphenyl MEH-PPV demonstrates the largest deviation in modulation depth as compared to defect-free MEH-PPV (see Figures 2C and 3B). The average value of the modulation for the 10% ortho-terphenyl MEH-PPV is still relatively high at 0.56, but the distribution of values is now much broader, with an almost equal probability of a polymer chain having a modulation depth anywhere from 0.1 to 1. This wide range of modulation depths suggest that, at 10% defect incorporation, the polymer chain can assume a wide variety of conformations ranging from nearly amorphous to highly folded.

Given the random nature of the chain-growth synthesis coupled with the low molecular weights of the compounds studied, the population of single molecules with high modulation depths may consist mainly of molecules with few, if any, defects. It is also possible that the 120° bend from the linear PPV backbone provided by the ortho-defect might enhance the ability of the chain to fold into a more compact, but still highly aligned structure. An example of such a structure can be seen in Figure 4C, where the regular placement of the ortho-terphenyl defects promotes alignment in the folded structure. However, in longer chains or at higher defect concentrations, it would be less likely that the random placement of these "kinks" would allow for such alignment. Indeed, the 30% ortho-terphenyl MEH-PPV compound demonstrated the lowest average modulation depth measured in this study, with a value of 0.40 (see Figure 3B). The distribution of modulation depth values is almost the exact opposite of the distribution of the 30% para-terphenyl MEH-PPV, with the majority of modulation depth values below 0.5. At 30% defect concentration, the majority of polymer chains now appear incapable of folding into the highly anisotropic structures that have been reported here and elsewhere. While most structures are likely to be adopting a more amorphous collapsed structure similar to a "molten globule" type conformation (see the first structure in Figure 4C), the modeled structure shown in Figure 5A demonstrates another possibility, wherein significant alignment in differing directions could offset one another. Another thing to consider is the tilt angle of the polymer molecules in the PMMA host. For a highly aligned, anisotropic polymer molecule, out-of-plane tilting will only decrease the observed modulation depth. However, in a polymer molecule with aligned regions with different orientations, the tilt angle of the molecule can either increase or decrease the modulation depth observed, perhaps explaining the tail to higher values for the highly defected ortho-terphenyl MEH-PPV.

In the simulations of 33% ortho-terphenyl MEH-PPV we observe an average radius of gyration of 12.1 Å, which is significantly lower than that of either the defect-free MEH-PPV or the para-terphenyl MEH-PPV. The anisotropy order parameter is similarly reduced, to a value of 0.75 and a modulation depth of 0.67. The observed trend of higher ortho-terphenyl defect concentrations to have lower modulation depths, more compact structures, and lower anisotropy values generally confirms our expectation that, at a high enough number of defects per chain, the folding of MEH-PPV into a highly aligned, anisotropic structure is disrupted.

Saturated Defect MEH-PPV. Results from the 10% saturated defect polymer (see Figure 2D) give an average modulation depth nearly identical to that measured for the defect-free MEH-PPV (0.69); however, the measured distribution is much sharper suggesting a more uniform distribution of conformations. Contrary to previous studies, our results suggest that the inclusion of a saturated backbone site at modest inclusion rates does not hinder highly anisotropic polymer folding[12] and may in fact enhance it in small quantities by adding a flexible hinge that enables the chain to fold into highly anisotropic rods.

In contrast, the modulation depth values for 30% saturated MEH-PPV (see Figure 3C) display a very broad and nearly static distribution between 0.2 and 0.9, with an average modulation depth value of 0.54. This distribution is quite similar to that of the 10% ortho-terphenyl MEH-PPV and characteristic of chains that adopt a wide array of morphologies. The data suggests that even at this high level of defect inclusion, it is still possible for chains to anisotropically fold; however, it is equally likely for chains to adopt a more disordered, isotropic conformation. This can be seen in the range of structures from the simulation shown in Figure 4D, where both a disordered collapsed structure and a highly anisotropic folded structure are shown. For these ~33% saturated defect MEH-PPV structures, the average radius of gyration is 20.5 Å, falling in between that of the ortho-terphenyl defect and the defect-free chain. The average anisotropy value is 0.87 with a corresponding modulation depth of 0.83, which are slightly higher than expected; however, the short chains explored in this simulation most likely bias the results toward more aligned structures since stiff segments of different lengths together can be better fit together when there are fewer segments.

The two-fold ability of this defect either to bend or to continue the linear chain is highlighted in Figure 5B, where four different saturated defects are circled. These defects show the range possible effects on the overall morphology. On the far left, a saturated defect induces a kink in the chain, enabling it to fold back on itself while still preserving the aligned nature of the straight chain. In the middle of the structure, there is a saturated defect in the top chain that is able to maintain its interaction with the defect-free segment of the lower chain, enhancing the stability of the anisotropic configuration. On the right, two saturated defects, one on each chain, have associated themselves such that the chains do not need to bend for them to continue their chain-to-chain association on the other side of the defects. Given this range of possible configurations for the saturated defect, short segments with even high proportions of saturated defects may remain highly anisotropic. However, when the alignment of the defects is less favorable, disordered structures, such as that shown on the left in Figure 4D, may result.

***Cis* Defects.** The substantial increase in *cis* defects in the ortho-terphenyl MEH-PPV and saturated MEH-PPV compounds as compared to the defect-free MEH-PPV and para-terphenyl MEH-PPV suggests that some kind of templating of the *cis* defect occurs during the chain growth synthesis of polymers with these two defects, due perhaps to the steric constraints imposed by these designed defects. The anticipated result is a decrease in the linearity of the backbone of the polymer, which is likely to then enhance the expected isotropic nature of these defected polymers. The 30% saturated MEH-PPV and 30% ortho MEH-PPV were refluxed with I_2 in toluene to convert the *cis* bonds to *trans*, resulting in compounds that contained only ~5% *cis* defect (see the Supporting Information).

Interestingly, with the removal of a majority of the *cis* defects, the 30% saturated MEH-PPV and 30% ortho MEH-PPV demonstrate identical solution absorption spectra and similar anisotropy histograms (see SI, Figures S3 and S4) with only the saturated defect compound showing only a minor shift in the anisotropy. The lack of significant structure change with the removal of *cis* defects is surprising and suggests a limitation in the role that intuition plays in predicting the how backbone defects can effect polymer morphology, especially in these already highly defected species.

The computational modeling results presented above neglect *cis* defects, instead focusing on chains with all *trans* linkages. The placement of *cis* linkages in the polymer is currently unknown, and given their higher concentrations in the more disordered polymers, it is likely that they are formed when two smaller chain segments are already associated with one another and can only be joined through a *cis* linkage. Thus, their placement may be poorly represented by random insertion in the simulated

Table 1. Incorporation of *cis* Double Bonds in MEH-PPV Backbone

polymer	% *cis*
MEH-PPV	5.3
10% ortho-terphenyl	18.7
30% ortho-terphenyl	13.1
10% saturated	19.0
30% saturated	15.1
10% para-terphenyl	5.8
30% para-terphenyl	7.6

structures, but how to bias their placement appropriately in our simulations is not clear. Even so, we performed additional simulations including *cis* defects at the frequencies shown in Table 1 on the same set of five probabilistically defected chains as examined for the *trans* case. As expected, the inclusion of *cis* linkages broadens the distributions of anisotropy values, such that they encompass more of the lower modulation depths observed experimentally, explaining in part why our calculated average modulation depth values are significantly higher than those measured experimentally. However, our set of *cis* structures is too small to represent well the combinatorial complexity that this additional structural defect introduces (see Supporting Information), and we thus focused here on the results of our all-*trans* simulations.

CONCLUSIONS

In summary, the linear nature of the para-terphenyl defects does not hinder efficient folding of the PPV chain and may in fact improve the alignment of the chromophores in the polymer at higher inclusion rates. The ortho-terphenyl defects provided the largest changes to the modulation depth data suggesting that, even at mild inclusion rates, these defects hinder chain alignment and at higher inclusion rates dramatically shift the single chain distribution toward less-ordered structures with lower anisotropies. The effect of the saturated defect, biphenylethane, on the single molecule anisotropy was surprisingly concentration-dependent; a low inclusion ratio results in a conformations with higher and more uniform anisotropies, while a high inclusion ratio results in a nearly equal probability of both low and high anisotropy conformations.

By combining synthetic, spectroscopic, and theoretical approaches we have laid the groundwork for being able to design polymer morphologies whereby the addition of different directing groups to the chain would influence the single molecule conformation of the conjugated polymer MEH-PPV in the manner desired. Single molecule measurements demonstrate that defect-free MEH-PPV and a linear defect that preserves the backbone geometry of PPV-type polymers results in highly anisotropic single molecule conformations, a highly bent defect results in a more isotropic conformation, and a defect that allows for rotational freedom of the backbone yields a concentration-dependent effect. At low concentrations, this defect still allows for anisotropic conformations. However, at higher concentrations it leads to chains that can adopt a wide range of conformations. Molecular dynamics simulations on model oligomeric systems show qualitative agreement with the experimental results, providing insight into the local folding induced by the different types of defects used in this study. Understanding polymer conformation at the single molecule level will lead to better insight into the role that morphology plays in conjugated polymer devices and how the properties of the individual components influence the characteristics of the bulk material.

ASSOCIATED CONTENT

Supporting Information. Complete procedures and details of the microscope apparatus, molecular dynamics and synthesis, NMR spectra, and additional figures. This material is available free of charge via the Internet at http://pubs.acs.org.

AUTHOR INFORMATION

Corresponding Author
jcb2873@mail.utexas.edu

ACKNOWLEDGMENT

This work was supported as part of the program "Molecular Tools for Conjugated Polymer Analysis and Optimization", a Center for Chemical Innovation (CCI, phase 1) under NSF Award No. CHE-0943957. We would like to thank Emilio Gallicchio for helpful conversations regarding the adjustment of the AGBNP potential for toluene, and Takuji Adachi for the use of his program in converting anisotropy values to modulation depth distributions.

REFERENCES

(1) Friend, R. H.; Gymer, R. W.; Holmes, A. B.; Burroughes, J. H.; Marks, R. N.; Taliani, C.; Bradley, D. D. C.; Dos Santos, D. A.; Bredas, J. L.; Logdlund, M.; Salaneck, W. R. *Nature* **1999**, *397*, 121–128.
(2) Ma, W. L.; Yang, C. Y.; Gong, X.; Lee, K.; Heeger, A. J. *Adv. Funct. Mater.* **2005**, *15*, 1617–1622.
(3) Mullen, K.; Swager, T. M. *Acc. Chem. Res.* **2008**, *41*, 1085–1085.
(4) Sivula, K.; Luscombe, C. K.; Thompson, B. C.; Frechet, J. M. J. *J. Am. Chem. Soc.* **2006**, *128*, 13988–13989.
(5) Adachi, T.; Brazard, J.; Chokshi, P.; Bolinger, J. C.; Ganesan, V.; Barbara, P. F. *J. Phys. Chem. C* **2010**, 20896–20902.
(6) Barbara, P. F.; Chang, W. S.; Link, S.; Scholes, G. D.; Yethiraj, A. *Annu. Rev. Phys. Chem.* **2007**, *58*, 565–584.
(7) Link, S.; Hu, D.; Chang, W. S.; Scholes, G. D.; Barbara, P. F. *Nano Lett.* **2005**, *5*, 1757–1760.
(8) Schwartz, B. J. *Annu. Rev. Phys. Chem.* **2003**, *54*, 141–172.
(9) Sumpter, B. G.; Kumar, P.; Mehta, A.; Barnes, M. D.; Shelton, W. A.; Harrison, R. J. *J. Phys. Chem. B* **2005**, *109*, 7671–7685.
(10) Vogelsang, J.; Brazard, J.; Adachi, T.; Bolinger, J. C.; Barbara, P. F. *Angew. Chem., Int. Ed.* **2011**, *50*, 2257–2261.
(11) Hu, D.; Yu, J.; Wong, K.; Bagchi, B.; Rossky, P. J.; Barbara, P. F. *Nature* **2000**, *405*, 1030–1033.
(12) Hu, D.; Yu, J.; Padmanaban, G.; Ramakrishnan, S.; Barbara, P. F. *Nano Lett.* **2002**, *2*, 1121–1124.
(13) Drury, A.; Maier, S.; Ruther, M.; Blau, W. J. *J. Mater. Chem.* **2003**, *13*, 485–490.
(14) Liao, L.; Pang, Y.; Ding, L. M.; Karasz, F. E. *Macromolecules* **2001**, *34*, 6756–6760.
(15) Pang, Y.; Li, J.; Hu, B.; Karasz, F. E. *Macromolecules* **1999**, *32*, 3946–3950.
(16) Yu, J.; Hu, D.; Barbara, P. F. *Science* **2000**, *289*, 1327–1330.
(17) Sugita, Y.; Okamoto, Y. *Chem. Phys. Lett.* **1999**, *314*, 141–151.
(18) Malkin, J. *Photophysical and Photochemical Properties of Aromatic Compounds* ; CRC Press: Boca Raton, FL, 1992; pp 103−106.